American Mineralogist, Volume 96, pages 188–196, 2011

Vorlanite ($CaU^{6+}O_4$)—A new mineral from the Upper Chegem caldera, Kabardino-Balkaria, Northern Caucasus, Russia

Evgeny V. Galuskin,[1,*] Thomas Armbruster,[2] Irina O. Galuskina,[1] Biljana Lazic,[2] Antoni Winiarski,[3] Viktor M. Gazeev,[4] Piotr Dzierżanowski,[5] Aleksandr E. Zadov,[6] Nikolai N. Pertsev,[4] Roman Wrzalik,[3] Anatoly G. Gurbanov,[4] and Janusz Janeczek[1]

[1]Faculty of Earth Sciences, Department of Geochemistry, Mineralogy and Petrography, University of Silesia, Będzińska 60, 41-200 Sosnowiec, Poland
[2]Mineralogical Crystallography, Institute of Geological Sciences, University of Bern, Freiestrasse 3, CH-3012 Bern, Switzerland
[3]August Chełkowski Institute of Physics, University of Silesia, Uniwersytecka 4, 40-007 Katowice, Poland
[4]Institute of Geology of Ore Deposits, Petrography, Mineralogy and Geochemistry (IGEM) RAS, Staromonetny 35, Moscow, Russia
[5]Institute of Geochemistry, Mineralogy and Petrology, University of Warsaw, al. Żwirki i Wigury 93, 02-089 Warszawa, Poland
[6]OOO Sci.-Research Center "NEOCHEM," Dmitrovskoye Highway 100/2, Moscow, Russia

Abstract

The new mineral vorlanite, ($CaU^{6+}O_4$), D_{calc} = 7.29 g/cm^3, H = 4–5, VHN_{10} = 360 kg/mm^2, was found near the top of Mt. Vorlan in a calcareous skarn xenolith in ignimbrite of the Upper Chegem caldera in the Northern Caucasus, Kabardino-Balkaria, Russia. Vorlanite occurs as aggregates of black platy crystals up to 0.3 mm long with external symmetry $\bar{3}m$. The strongest powder diffraction lines are [*d*(Å)/(*hkl*)]: 3.107/(111), 2.691/(200), 1.903/(220), 1.623/(311), 1.235/(331), 1.203/(420), 1.098/(422), 0.910/(531). Single-crystal X-ray study gives isometric symmetry, space group $Fm\bar{3}m$, a = 5.3813(2) Å, V = 155.834(10) Å^3, and Z = 2. X-ray photoelectron spectroscopy indicate that all U in vorlanite is hexavalent. The mineral is isostructural with fluorite and uraninite ($U^{4+}O_2$). In contrast to synthetic rhombohedral $CaUO_4$, and most U^{6+} minerals, the U^{6+} cations in vorlanite are present as disordered uranyl ions. $^{[8]}Ca^{2+}$ and $^{[8]}U^{6+}$ are disordered over a single site with average M-O = 2.33 Å.

Vorlanite is believed to be a pseudomorphic replacement of originally rhombohedral $CaUO_4$. We assume that this rhombohedral phase transformed by radiation damage to cubic $CaUO_4$ (vorlanite). The new mineral is associated with larnite, chegemite, reinhardbraunsite, lakargiite, rondorfite, and wadalite, which are indicative of high-temperature formation (>800 °C) at shallow depth.

Keywords: Vorlanite, $CaUO_4$, uranium, skarn, structure, Raman, XPS, Lakargi

Introduction

Vorlanite ($CaU^{6+}O_4$ [fluorite-type structure, $Fm\bar{3}m$, a = 5.3813(2) Å, V = 155.834(10) Å^3] was found in 2008 in high-temperature skarns in the calcareous xenolith no. 7, hosted by ignimbrites of the Upper Chegem caldera in the Northern Caucasus, Kabardino-Balkaria, Russia. Vorlanite is another new mineral from altered xenoliths dispersed between Mt. Lakargi and Mt. Vorlan (coordinates 43°17′N 43°6.42′E; see geological map in Galuskin et al. 2009). They include calcio-olivine Ca_2SiO_4 (Zadov et al. 2008), lakargiite $CaZrO_3$ (Galuskin et al. 2008), chegemite $Ca_7(SiO_4)_3(OH)_2$ (Galuskin et al. 2009), kumtyubeite $Ca_5(SiO_4)_2F_2$ (Galuskina et al. 2009), toturite $Ca_3Sn_2Fe_2SiO_{12}$ (Galuskina et al. 2010a), elbrusite-(Zr) $Ca_3ZrU^{6+}Fe_2^{3+}Fe^{2+}O_{12}$ (Galuskina et al. 2010b), bitikleite-(SnAl) $Ca_3SbSnAl_3O_{12}$ and bitikleite-(ZrFe) $Ca_3ZrSbFe_3O_{12}$ (Galuskina et al. 2010c), $KNa_2Li(Mg,Fe)_2Ti_2Si_8O_{24}$ (IMA2009-009), and $CaSnO_3$ (IMA2009-090).

Vorlanite stoichiometry is identical with the synthetic rhombohedral calcium uranate $CaUO_4$. However, while hexavalent uranium in the latter has characteristic 2+6 coordination of oxygen, as known for the uranyl ion $(U^{6+}O_2)^{2+}$ (Loopstra and Rietveld 1969), the U^{6+} cation in vorlanite is eightfold coordinated by equidistant O atoms, which is typical of the fluorite-type structure. In this respect, vorlanite is exceptional among U^{6+} minerals because the great majority of them show order of linear $(U^{6+}O_2)^{2+}$ uranyl ions (Burns 1999, 2005).

Vorlanite, named after Mt. Vorlan, was approved as a new mineral species by CNMNC IMA in July 2009 (IMA2009-032). The type specimen of vorlanite is deposited in the Fersman Mineralogical Museum in Moscow, Russia (catalog no. 3838/1). In this paper we provide a detailed description of vorlanite.

Methods of investigations

Crystal morphology and chemical composition of vorlanite and associated minerals were examined using optical microscopes, analytical electron scanning microscope Philips XL30 ESEM/EDAX (Faculty of Earth Sciences, University of Silesia) and electron microprobe CAMECA SX100 (Institute of Geochemistry, Mineralogy and Petrology, University of Warsaw). Electron-microprobe analyses of vorlanite were performed at 15 kV and 40–50 nA using the following lines and standards: U*M*β for synthetic UO_2, Ca*K*α for wollastonite and diopside; Fe*K*α for hematite.

Raman spectra of single crystals of vorlanite were recorded using LabRAM HR800 (Jobin-Yvon-Horiba, Wrocław University of Technology) equipped with an 1800 line/mm grating monochromator, a charge-coupled device (CCD) Peltier-

* E-mail: evgeny.galuskin@us.edu.pl

cooled detector (1024 × 256), and an Olympus BX40 confocal microscope. Incident laser excitation was provided by a water-cooled argon laser source operating at 514.5 nm. The power at the exit of a 100× objective lens varied from 40 to 60 mW. The Raman spectra were recorded in 0° degree geometry, in the range of 50–4000 cm^{-1} Raman shift and with spectral resolution of 2.5 cm^{-1}. Collection time of 10 s and accumulation of 16 scans were chosen. The monochromator was calibrated using the Raman scattering line of a silicon plate (520.7 cm^{-1}).

Structural data of vorlanite were collected with an APEX II SMART single-crystal diffractometer (University of Bern), Mo$K\alpha$, $\lambda = 0.71073$ Å, operated at 50 kV and 35 mA. X-ray powder diffraction data were obtained using a diffractometer D/max RAPID II-R Rigaku 2D (August Chełkowski Institute of Physics, University of Silesia) equipped with imaging plate, using Bragg-Brentano geometry, 60 kV, 200 mA, collimator 0.1 mm, Ag$K\alpha_{1+2}$, $\lambda = 0.559420$ Å, and 0.563811 Å. Vorlanite grains used for structural investigations were plucked out from the fresh surface of the sample using a steel needle. The homogeneity of vorlanite crystals for single-crystal X-ray study was checked using a scanning electron microscope. Vorlanite grains for powder diffraction investigation were crushed with a glass slide without grinding and subsequently rolled up with gum arabic to a small sphere (0.28 mm in size).

The X-ray photoelectron spectroscopy (XPS) measurements were performed with a multipurpose electron spectrometer PHI5700/660 from Physical Electronics (August Chełkowski Institute of Physics, University of Silesia), using monochromatic Al$K\alpha$ (1486.6 eV) radiation with a spot size of 120 µm and a hemispherical energy analyzer. The anode was operated at 15 kV and 225 W. The high-resolution spectra were collected with 23.50 pass energy, corresponding to an energy resolution of about 0.1 eV (step 0.10 eV, time 100 ms). The binding energies were calibrated by fixing the C1s peak (adventitious carbon) at 285.0 eV. High-resolution spectra were fitted using mixed Gaussian and Lorentzian functions and Shirley background with help of MultiPak program.

Mineral association, morphology, and physical properties of vorlanite

The vorlanite-bearing xenolith no. 7 of heavily altered skarn is some 5 m in diameter and crops out 500 m south of the top of Mt. Vorlan (see map in Galuskin et al. 2009). Vorlanite is an accessory mineral in the skarn composed of millimeter-sized lenses of larnite with rondorfite and wadalite inclusions. Larnite occurs partially replaced by chegemite, reinhardbrausite, and minerals of the fluorellestadite-hydroxylellestadite series. White-grayish lenses of larnite are embedded in the yellow mass of secondary katoite-hibschite, afwillite, hillebrandite, bultfonteinite, hydrocalumite, ettringite group minerals, and spots of minute hematite. Vorlanite is locally associated with elbrusite-(Zr), U-bearing lakargiite, perovskite, and srebrodolskite.

Skarns with abundant secondary low-temperature minerals are enriched in vorlanite, potentially suggestive of vorlanite being a low-temperature mineral (Fig. 1a). However, rare vorlanite occurrences in only slightly altered rock fragments, together with other high-temperature minerals such as larnite, chegemite, reinhardbraunsite, rondorfite, wadalite, fluor- and hydroxylellestadite (Fig. 1b) confirm vorlanite's high-temperature genesis.

Platy crystals up to 300 µm across and 15–20 µm thick of vorlanite commonly form sheaves (Fig. 1a–1b). Vorlanite crystals have xenomorphic form with rare outgrowths of platelets having hexagonal outlines (Fig. 1c). Basal pinacoids display a stepped growth micro-relief due to stacking of hexagonal plates (Fig. 1d) or are characterized by growth of thin hexagonal layers (Fig. 1e), which suggests point group symmetry $\bar{3}m$ (trigonal) for the morphology of vorlanite.

Vorlanite crystals are usually deformed, they are often bent and highly fractured (Fig. 1c). In addition, formation of microblocks along cracks is observed (Fig. 1e). Usually, the central part of vorlanite crystals is distinguished by increased porosity (Fig. 1f). Square and triangular pore shape suggests that the pores were formed as a result of wadalite and rondorfite dissolution. Corresponding unaltered inclusions were also detected in vorlanite. A few crystals are highly deformed and <5 µm thick (Figs. 2a–2c). Elongated blocks in vorlanite crystals have irregular, dendritic form with cross-sections <600 nm in size.

Vorlanite is black with submetallic luster and dark brown to cherry-red streak, which gives it a superficial resemblance to hematite. In thin section it is translucent, brownish-red. Vorlanite is optically isotropic. In reflected light it is light-gray with brown or red internal reflections. Unfortunately, we are unable to measure the refractive index of vorlanite and to collect a full reflectance spectrum. Reflectance values measured in oil with $n = 1.518$ are: 10.4(3) for 589 nm; 10.6(3) for 470 nm; 9.7(5) for 650 nm; 11.3(1) for 546 nm (synthetic ZnS and coal with reflectivity of 5.5% were used as standards).

The Mohs hardness is 4–5 and the microhardness is VHN_{10} = 360 kg/mm^2. Vorlanite is brittle. Its density calculated from the empirical formula and cell volume is 7.29 g/cm^3. Vorlanite is radioactive and as a result of its radioactivity it is surrounded by easily visible pleochroic haloes up to 20–25 µm wide in the inclosing silicates.

The new mineral dissolves in 10% HCl at room temperature. The basal pinacoid with visible growth layers was etched with 2% HCl, which brought out traces of alpha-particle tracks (Fig. 2d). The tracks, sub-perpendicular to the surface, show square etch holes from 150 to 200 nm in size (Fig. 2e).

Chemical composition and crystal structure of vorlanite

The chemical composition of vorlanite is identical with synthetic calcium uranate $CaUO_4$ (Table 1). However, from X-ray single-crystal diffraction the space group of vorlanite is $Fm\bar{3}m$ (Table 2); whereas synthetic $CaUO_4$ is rhombohedral, space group $R\bar{3}m$ (Zachariasen 1948; Loopstra and Rietveld 1969). In addition, it is not possible to transform the cubic $Fm\bar{3}m$ lattice with $a = 5.3813(2)$ Å (this study) into a trigonal cell with a = 6.2683 Å, $\alpha = 36.04°$ (rhombohedral setting), $a = 3.8782$, c = 17.564 Å (hexagonal setting) or vice versa. The single-crystal diffraction pattern of vorlanite is sharp without any indication of metamictization and without any additional reflections not corresponding to the observed F-centered cubic lattice. The crystal structure refinement of vorlanite revealed it to be isostructural with uraninite (UO_2), i.e., fluorite-type structure (Tables 2–4). CIFs are deposited[1]. In vorlanite U^{6+} and Ca^{2+} cations randomly occupy the eightfold-coordinated site with a metal (M) to oxygen (O) distance M-O = 8 × 2.3302 Å (Table 4). In the ordered structure of rhombohedral $CaUO_4$, uranium and calcium occupy two different eightfold-coordinated sites, with Ca-O(1) = 6 × 2.4377 Å and Ca-O(2) 2 × 2.4116 Å. The UO_8 coordination polyhedron has U-O(2) = 6 × 2.2977 Å and U-O(1) 2 × 1.9637 Å (Loopstra and Rietveld 1969, who incorrectly reported fivefold coordination for Ca).

[1] Deposit item AM-11-012, CIFs. Deposit items are available two ways: For a paper copy contact the Business Office of the Mineralogical Society of America (see inside front cover of recent issue) for price information. For an electronic copy visit the MSA web site at http://www.minsocam.org, go to the *American Mineralogist* Contents, find the table of contents for the specific volume/issue wanted, and then click on the deposit link there.

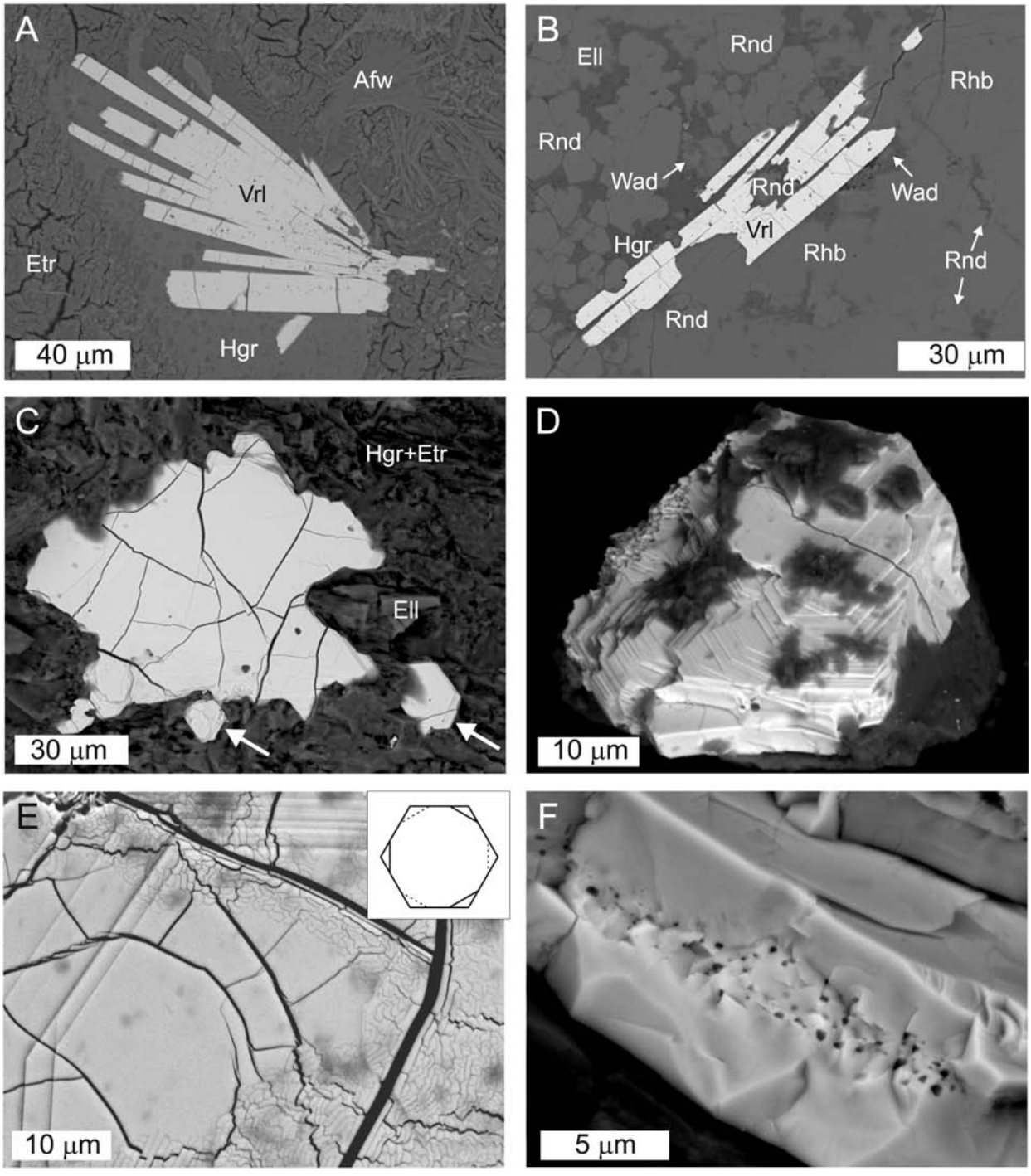

Figure 1. (**a**) Sheaves of platy vorlanite crystals in highly altered skarn, (**b**) intergrowth of platy vorlanite crystals in weakly altered skarn, (**c**) xenomorphic vorlanite crystal with platelets outgrowths with hexagonal outlines (indicated by arrows), (**d**) platy vorlanite crystal with a stepped micro-relief of stacked hexagonal plates on the basal pinacoid, (**e**) hexagonal growth layers on the basal pinacoid of vorlanite, blocks developing along fractures are well visible. In inset: model of microrelief on upper (solid line) and lower (dashed line) basal pinacoids, (**f**) platy vorlanite crystal displaying increased porosity in the center. BSE images: (**a**, **b**) high vacuum; (**c**–**f**) low vacuum, 0.3 Torr, without coating. Etr = ettringite, Vrl = vorlanite, Awf = awfillite, Rnd = rondorfite, Wad = wadalite, Rhb = reinhardbraunsite, Ell = hydrohylellestadite, Hgr = hibschite.

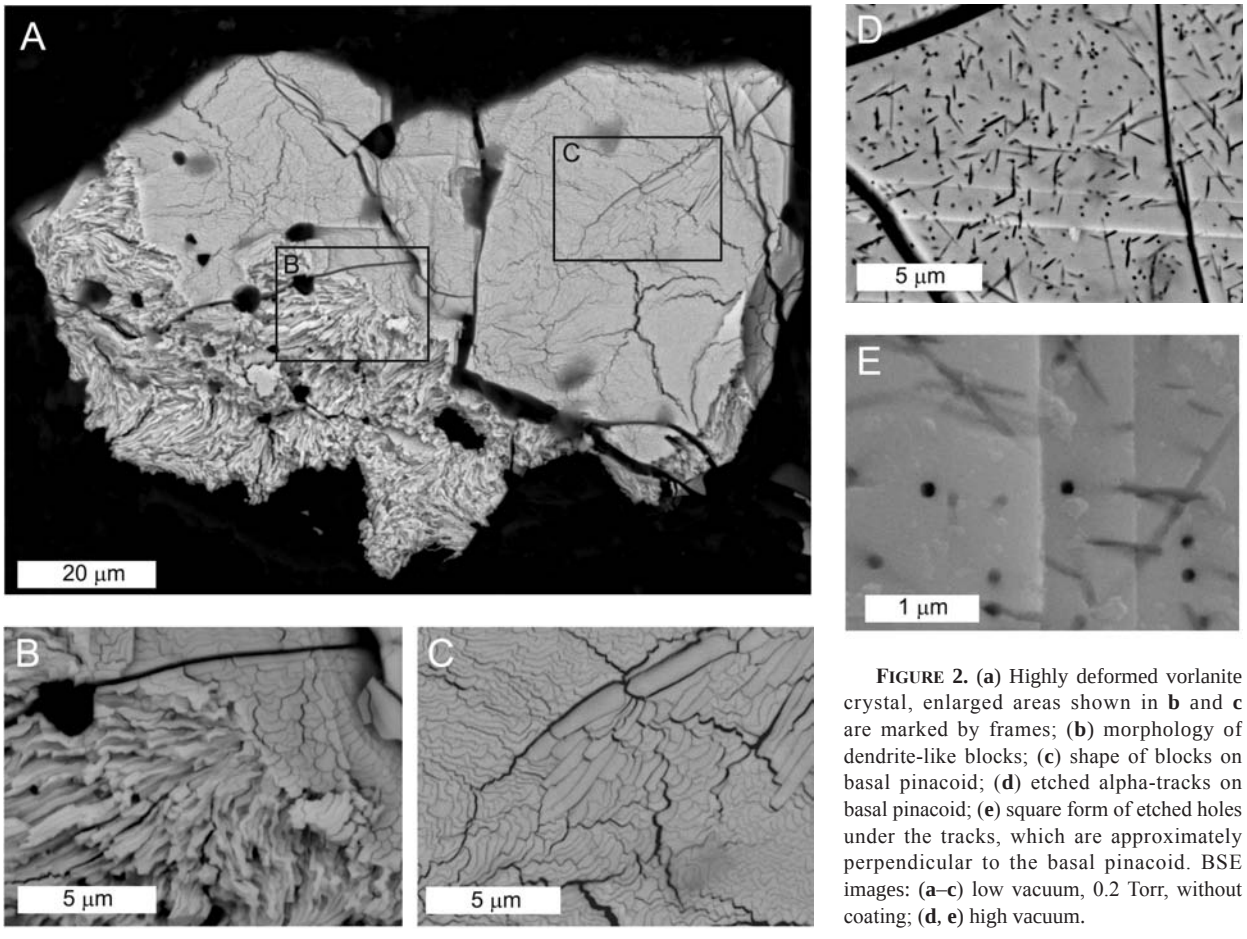

FIGURE 2. (**a**) Highly deformed vorlanite crystal, enlarged areas shown in **b** and **c** are marked by frames; (**b**) morphology of dendrite-like blocks; (**c**) shape of blocks on basal pinacoid; (**d**) etched alpha-tracks on basal pinacoid; (**e**) square form of etched holes under the tracks, which are approximately perpendicular to the basal pinacoid. BSE images: (**a**–**c**) low vacuum, 0.2 Torr, without coating; (**d**, **e**) high vacuum.

TABLE 1. Electron microprobe analysis of vorlanite

	Mean 36	St. dev.	Range
UO_3 wt%	84.06	0.48	82.76–84.84
CaO	16.65	0.15	16.39–17.04
Fe_2O_3	0.06	0.06	0–0.20
Total	100.77	0.51	99.54–101.74
	Calculated on two cations		
Ca	1.002	0.006	0.989–1.013
U^{6+}	0.995	0.007	0.982–1.008
Fe^{3+}	0.003	0.003	0–0.008
Dα*	6.30×10^{15}		
dpa	0.56		

* See explanation in text.

TABLE 2. Data collection and structure refinement details for vorlanite

Temperature	296(2) K
Theta range for data collection	6.57 to 32.99°
Index ranges	$-7 \le h \le 8, -8 \le k \le 8, -8 \le l \le 8$
Reflections collected	1548
Independent reflections	29 (R_{int} = 0.0329)
Crystal size	0.01 × 0.03 × 0.05 mm
Crystal system	cubic
Space group	$Fm\bar{3}m$
Unit-cell dimensions	a = 5.3813(2) Å
V	155.834(10) Å^3
Z	2
D(calc)	7.291 g/cm^3
Goodness-of-fit on F^2	1.322
Final R indices	29 data; $I > 2\sigma(I)$, $R1$ = 0.0083
	all data $R1$ = 0.0083, $wR2$ = 0.0190
Largest diff. peak and hole	0.260 and –0.358 eÅ^{-3}

TABLE 3. Atomic coordinates and equivalent isotropic atomic displacement parameters (Å^2) for vorlanite

Atom	*x/a*	*y/b*	*z/c*	U_{eq}	Occ.
U1	0.0000	0.5000	0.0000	0.0179(2)	0.47(2)
Ca1	0.0000	0.5000	0.0000	0.0179(2)	0.53(2)
O1	0.2500	0.2500	0.2500	0.057(3)	1

Note: All atoms at special positions: $U_{11} = U_{22} = U_{33} = U_{eq}$, $U_{12} = U_{13} = U_{23} = 0$. U_{eq} is defined as one third of the trace of the orthogonalized U_{ij} tensor.

TABLE 4. Bond lengths (Å) and angles (°) for vorlanite

Atoms			Bond length (Å)	Mult.
U1	O1		2.3302*	×8
Ca1	O1		2.3302	×8
Ca1	U1		3.8052(1)	×4
Atoms			Angle (°)	Mult.
O1	U1	O1	180.0	×4
O1	U1	O1	109.5	×12
O1	U1	O1	70.5	×12

* E.s.d. values of bond lengths are smaller than the last dig it cited. All atoms are on special position.

The cubic symmetry of vorlanite was confirmed by X-ray powder diffraction [a = 5.381(1) Å, V = 155.81(1) Å^3, Z = 2; Table 5; Fig. 3]. No peaks of the rhombohedral $CaUO_4$ phase were detected in the X-ray diffraction pattern of vorlanite (Fig. 3).

The single-crystal X-ray structure refinements of vorlanite were performed with different assumptions. First, the occupancies of Ca and U were allowed to vary, but not O. After the refinement confirmed (within 1.5 e.s.d. values) the analytically

TABLE 5. XRD powder data for vorlanite (Ag*K*α)

hkl	d_{calc}/Å*	d_{obs}/Å	I_{calc}	I_{obs}	*hkl*	d_{calc}/Å	d_{obs}/Å	I_{calc}	I_{obs}
111	3.107	3.105	100.0	100	711	0.754	0.754	4.7	9
200	2.691	2.690	29.5	34	551	0.754		4.7	
220	1.903	1.905	63.2	60	640	0.746	0.745	3.4	4
311	1.623	1.623	54.4	54	642	0.719	0.719	10.2	7
222	1.553	1.557	10.3	13	731	0.701	0.704	7.2	8
400	1.345	1.345	10.9	11	553	0.701		3.6	
331	1.235	1.235	24.1	22	733	0.657	0.657	2.8	4
420	1.203	1.203	15.5	21	644	0.653	0.653	2.1	4
422	1.098	1.099	22.3	22	820	0.653		2.1	
333	1.036	1.036	4.6	20	822	0.634	0.636	3.2	4
511	1.036		13.8		660	0.634		1.6	
440	0.951	0.949	6.9	6	751	0.621	0.621	4.6	5
531	0.910	0.910	18.1	17	662	0.617	0.617	1.7	2
600	0.897	0.899	1.6	13	840	0.602	0.602	2.6	2
442	0.897		6.4		753	0.591	0.592	3.8	5
620	0.851	0.852	9.3	9	911	0.591		1.9	
533	0.821	0.818	6.4	6	842	0.587	0.585	2.8	2
622	0.811	0.809	4.6	4	664	0.574	0.574	2.2	2
444	0.777	0.777	2.2	3	931	0.564	0.564	3.1	3

*E.s.d. values of d_{obs} and d_{calc} are smaller than the last digit cited.

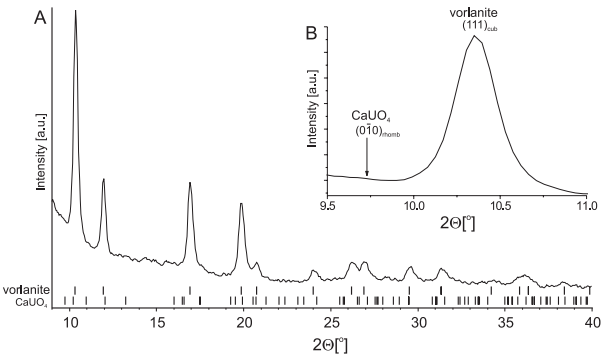

FIGURE 3. Powder X-ray diffraction pattern of vorlanite (Ag*K*α radiation) (**a**), bars indicate peak positions of vorlanite and rhombohedral $CaUO_4$ as subscript, enlarged portion indicating that a strong peak (relative intensity ~70%) from rhombohedral $CaUO_4$ is absent (**b**).

determined Ca/U ratio of 1/1 (Table 3), the occupancies were fixed at 0.5 U and 0.5 Ca, and the population of oxygen was allowed to vary to determine whether there were significant anion vacancies characteristic of U with valence <6+. Subsequent refinements converged to an oxygen occupancy of 1.03(3), excluding significant oxygen vacancies. Thus, results of the structural refinements require that all U in vorlanite is U^{6+}, and the final refinement assumed full occupancy at the O sites (Table 3).

To confirm that U in vorlanite is hexavalent, we additionally recorded an XPS spectrum (Fig. 4) from a fresh natural surface of the crystal shown in Figure 1c. An aperture of 120 μm in diameter was used, thus the beam also struck the adjacent matrix. However, this did not disturb collection of a qualitative spectrum in the area of U4f bond energy (Fig. 4a) as surrounding minerals do not contain uranium. Peaks of U4f in the XPS spectrum of vorlanite have small full-width at half maximum (FWHM) ~1.5 eV, allowing a peak fit with only one curve (Fig. 4a). If the positions of U4f peaks and their satellites in vorlanite are compared with known XPS data of other U-phases it is evident that U in vorlanite occurs only as U^{6+}. Line $U4f_{5/2}$ responds to bond energy 392.3 eV and line $U4f_{7/2}$ responds to 381.5 eV (Fig. 4a), which is significantly higher than the bond energies for U^{5+} and U^{4+} (Bera et al. 1998; Van den Berghe et al. 2000; Collela et al. 2005; Liu et al. 2009; Schindler et al. 2009). Furthermore, bond energies in vorlanite are equal to those in the uranates $SrU^{6+}O_4$ and $Sr_3U^{6+}O_6$ ($Uf4_{7/2}$ = 381.5 eV, $Uf4_{5/2}$ = 392.3 eV) (Allen et al. 1978). Interestingly, bond energies of synthetic oxygen-deficient rhombohedral $CaUO_{4-x}$ differ and are slightly lower than those of vorlanite: $Uf4_{7/2}$ = 381.1 eV and $Uf4_{5/2}$ = 391.8 eV (Allen et al. 1978). Even lower values $Uf4_{7/2}$ = 380.7 ± 0.2 eV and $Uf4_{5/2}$ = 391.5 ± 0.2 eV have been found for stoichiometric rhombohedral uranate $CaUO_4$ (Chadwick 1973). The separation between the two main peaks $Uf4_{5/2}$ and $Uf4_{7/2}$ in the XPS spectrum of vorlanite is 10.8 eV, which is characteristic of the majority of uranium compounds (Schindler et al. 2009), whereas the distances between the main peaks and their satellites in vorlanite are smaller than corresponding values in known data of U-phases (Fig. 4a). As an example, the distances between the main peak $Uf4_{5/2}$ and the two satellites in the vorlanite spectrum are 9.2 and 2.5 eV (Fig. 4a), respectively. Corresponding values of 10 and 4 eV have been determined for the uranate $Cs_4U^{6+}_5O_{17}$ (Van den Berghe et al. 2000) and for peaks of U^{+6} in partially oxidized uraninite UO_{2+x} (Schindler et al. 2009). For oxygen-deficient $CaUO_{4-x}$ there are no data for the 4 eV-type satellite but the second satellite is

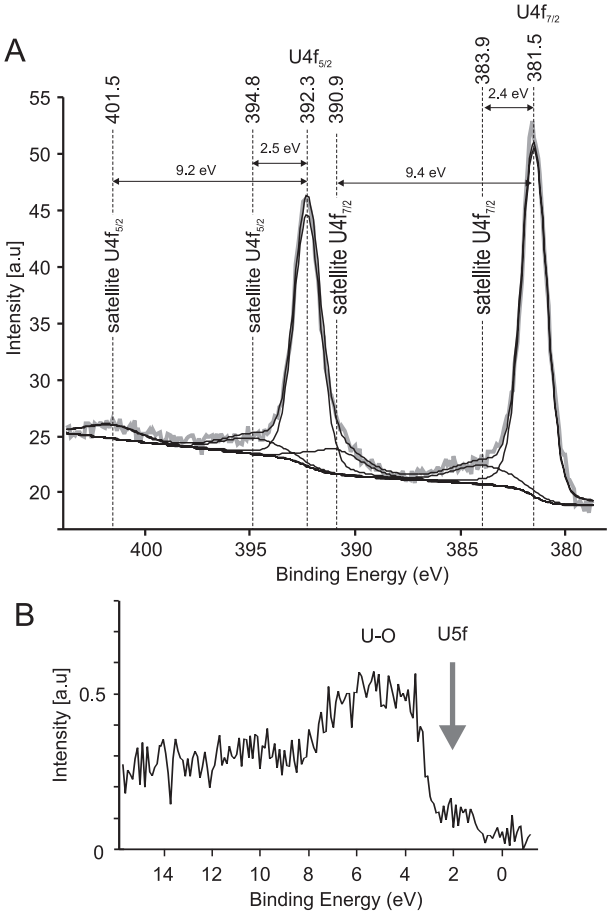

FIGURE 4. X-ray photoelectron spectra of vorlanite in the U4f region (**a**) and U5f valence band region (**b**).

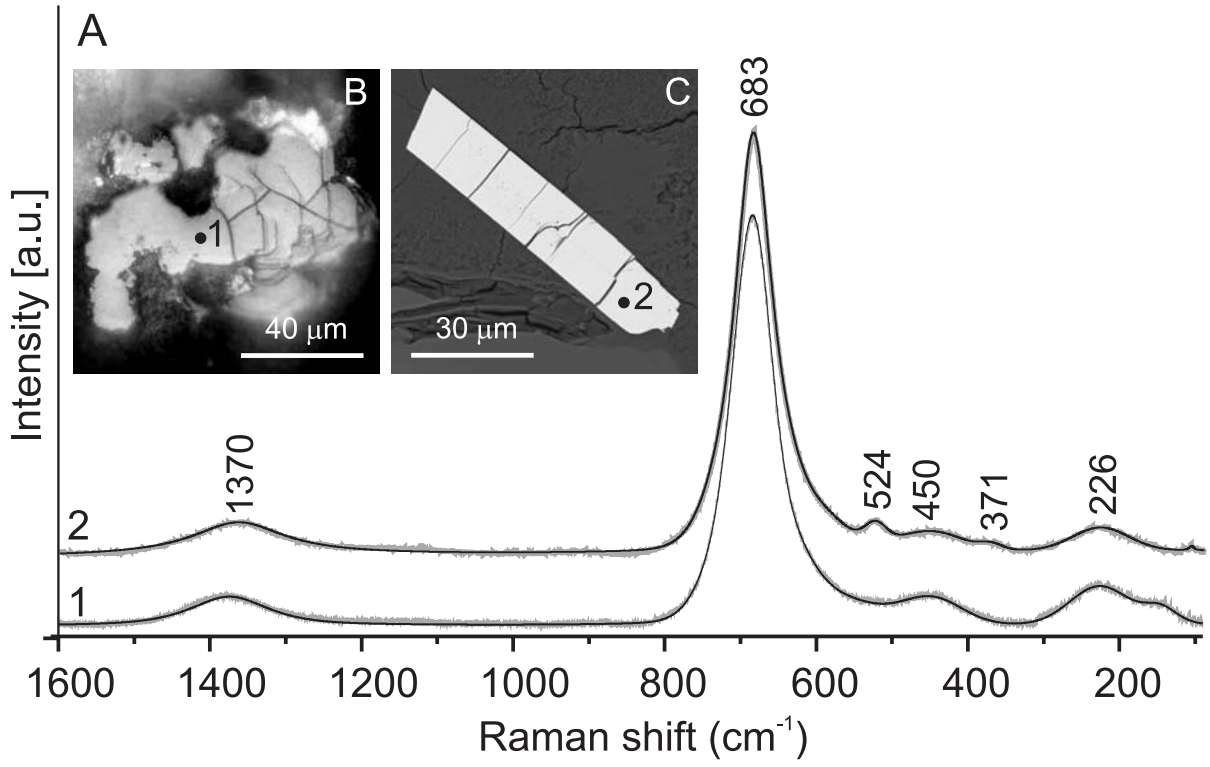

FIGURE 5. Raman spectra of vorlanite obtained from basal pinacoid (spectrum 1, inset: **b**, reflected ligth) and from crystal cross-section approximately perpendicular to basal pinacoid in thin section (spectrum 2, inset: **c**, BSE image).

within 9.4 eV (Allen et al. 1978), which is very close to value obtained for vorlanite (Fig. 4a). The U5f peak is not observed in the valence band XPS spectrum of vorlanite (–2 to 16 eV), validating that all U is hexavalent (Fig. 4b; Van den Berghe et al. 2000; Schindler et al. 2009).

Raman spectra of vorlanite were obtained: (1) for a natural pinacoid crystal surface, and (2) for a grain from a thin section, oriented sub-perpendicular to the pinacoidal face (Fig. 5). Intensities of absorption bands in the spectra of vorlanite are one or two orders of magnitude smaller than for the associated silicate minerals. The main absorption band at 683 cm^{-1} is the major feature in the Raman spectra of vorlanite (Fig. 5). The position of that band is close to the band at 696 cm^{-1} related to uranyl UO_2^{2+} symmetric (ν_s) stretching vibrations in the rhombohedral $CaUO_4$, which corresponds to the interatomic distance U-O_I = 1.964 Å (Loopstra and Rietveld 1969; Liegeois-Duyckaerts 1977; Allen and Griffiths 1979). In the Raman spectrum of rhombohedral $CaUO_4$ (eight-coordinated U^{6+}, U-O_I = 1.964 Å) the band at 696 cm^{-1} (ν_s) is shifted to lower frequencies compared to spectra of other monouranates, for example, $SrUO_4$ at 737 cm^{-1} (six-coordinated U^{6+}, U-O_I = 1.85 Å) and $BaUO_4$ at 726 cm^{-1} (six-coordinated U^{6+}, U-O_I = 1.89 Å) (Allen and Griffiths 1979).

Calculated active modes for monouranates based on analysis of layer forming $[(UO_2)O_2]^{2-}$ units gave values ν_s close to those determined for vorlanite, for example K_2UO_4 at 686 cm^{-1} [six-coordinated U^{6+}, U-O_I = 1.913(6) Å] (Ohwada 1970; Roof et al. 2010). Calculation of interatomic U-O_I distances for uranyl ions using the empirical formula $R_{U-OI} = a + b[\nu_s(U)O)_2^{2+}]^{-2/3}$ Å, where a = 0.575, b = 106.5 (Bartlett and Cooney 1989) yields for vorlanite R_{U-OI} = 1.948 Å, and for rhombohedral $CaUO_4$ R_{U-OI} = 1.931 Å, which is too short compared to 1.964 Å as calculated from structural data of rhombohedral $CaUO_4$ (Loopstra and Rietveld 1969). Based on the structural data for rhombohedral $CaUO_4$ (Loopstra and Rietveld 1969; Liegeois-Duyckaerts 1977; Allen and Griffiths 1979), we slightly modified the equation of Bartlett and Cooney (1989) deriving a new coefficient b = 109.11. Subsequently, the revised empirical formula yielded an improved interatomic distance U-O_I – R_{U-OI} = 1.982 Å for vorlanite.

The Raman spectrum of rhombohedral $CaUO_4$ has two strong bands: 696 and 534 cm^{-1} and two medium intensity bands: 379 and 340 cm^{-1} (Liegeois-Duyckaerts 1977; Allen and Griffiths 1979). The Raman spectrum of vorlanite has only one strong band at 683 cm^{-1} (Fig. 5). Interpretation of additional bands in the vorlanite spectrum is ambiguous because of their weak intensity and broad width (Fig. 5). Bands near 524 and 450 cm^{-1} may be related to U-O_{II} stretching vibrations in the $[UO_8]$ unit for U-O >2.2 Å distances (Hoekstra 1965; Volkovich et al. 1998, 2001). A very weak and diffuse band near 371 cm^{-1} may correspond to Ca-O vibrations, whereas a weak band near 226 cm^{-1} may be associated with an U-O_I bending mode (Hoekstra 1965; Volkovich et al. 1998, 2001).

The band at 1370 cm^{-1} is most probably an overtone (683 cm^{-1} × 2 = 1366 cm^{-1}). However, a band at 1360 cm^{-1} was described but not interpreted in Raman spectra collected on a (111) face of an

UO_2 single crystal (Senanayake et al. 2005). There are no absorption bands in the OH region of the vorlanite Raman spectrum.

Results of the Raman study on vorlanite add important information to the structural data. X-ray diffraction refinement of the vorlanite structure locates U at an eight-coordinated site (ideal cube) with equivalent U-O = 2.3302 Å distances (Table 3), whereas Raman data indicate that there are short U-O bonds ($R_{U\text{-}O} \approx 1.98$ Å) characteristic of the uranyl ion present in vorlanite. That is, the X-ray refinement gives an average structure, whereas the Raman spectra reveal the existence of uranyl ions not evident in the average structure and demonstrate thereby an important similarity of vorlanite to rhombohedral $CaUO_4$.

Discussion

Vorlanite is distinctive because its black color is not characteristic of a compound with hexavalent uranium (Grenthe et al. 2006) and because its trigonal ($\bar{3}m$) morphology does not match the cubic symmetry (space group $Fm\bar{3}m$) revealed by X-ray diffraction. Moreover, two very different cations Ca^{2+} and U^{6+} are statistically accommodated in a ~1:1 ratio at the same structural site. How could a mineral with such unexpected features have formed and what does define its stability or metastablity?

A strong similarity in color between vorlanite and hematite is noted: black color for big and thick crystals and dark-red, cherry color for thin crystals and powder. Dark-red color was also noted for cubic δ-UO_3 (Belle 1961).

The discrepancy in symmetry between morphology and structure suggests that vorlanite is a pseudomorph (or more precisely paramorph), most plausibly, after rhombohedral calcium uranate and formed as a product of phase transition. X-ray single-crystal diffraction data indicate that vorlanite crystals are true monocrystals.

The vorlanite structure may be derived directly from uraninite, nominally UO_2, by substituting half of the U^{4+} cations by U^{6+} and the other half of U^{4+} by Ca^{2+} according to the scheme proposed for partially oxidized and impure uraninites: $2U^{4+} \leftrightarrow Ca^{2+}U^{6+}$ (Janeczek and Ewing 1992). However, the smaller cell dimension of vorlanite (a = 5.38 Å) compared to pure UO_2 (a = 5.47 Å) cannot be entirely explained by a simple substitution of 0.5 U^{6+} (ionic radius of 0.86 Å) + 0.5 Ca (1.12 Å) for U^{4+}. Although this replacement gives a mean cation radius (0.99 Å) essentially equal to the ionic radius of U^{4+} (1.00 Å; Shannon 1976) in uraninite, the (Ca,U^{6+})-O distance of 2.33 Å in vorlanite is significantly shorter than the U^{4+}-O distance (2.37 Å) in uraninite. The large difference in ionic radii and charges between $^{[8]}U^{6+}$ and $^{[8]}Ca^{2+}$ would be expected to exert significant stress on the cubic vorlanite structure, but we have not seen any anomalous optical anisotropy typical of strained structures. It could well be that vorlanite is a metastable phase.

Structures of vorlanite and rhombohedral synthetic $CaUO_4$ are not so different as they might appear at first glance (Fig. 6). The structure of rhombohedral $CaUO_4$ can also be derived from the CaF_2 fluorite structure (Zachariasen 1948; Matar and Demazeau 2009). Layers of deformed coordination cubes of the two types (Ca and U) are arranged in rhombohedral $CaUO_4$ perpendicular to the $\bar{3}$-fold axis (= direction of uranyl bond). In rhombohedral $CaUO_4$, Ca^{2+} and U^{6+} have ordered distribution (Fig. 6a). The layers of ideal cubes in vorlanite are also arranged perpendicular to the $\bar{3}$-fold axes (four variants of orientation are possible). However, Ca^{2+} and U^{6+} have disordered distribution in vorlanite (Fig. 6b). In vorlanite eight oxygen atoms form a regular cube-like coordination of U^{+6} (and Ca), whereas in rhombohedral synthetic $CaUO_4$ the corresponding cube is distorted with one body diagonal of 2×1.96 Å and the remaining three of 2×2.30 Å (Fig. 6a). Mean interatomic M-O distances for vorlanite and rhombohedral synthetic $CaUO_4$ are very similar, 2.33 and 2.32 Å, respectively. Atomic displacement parameters in vorlanite are fairly high (Table 3) as expected for a strongly disordered structure. In particular, U of oxygen in vorlanite is one order of magnitude larger than the corresponding U (cited as $B = 8\pi^2$

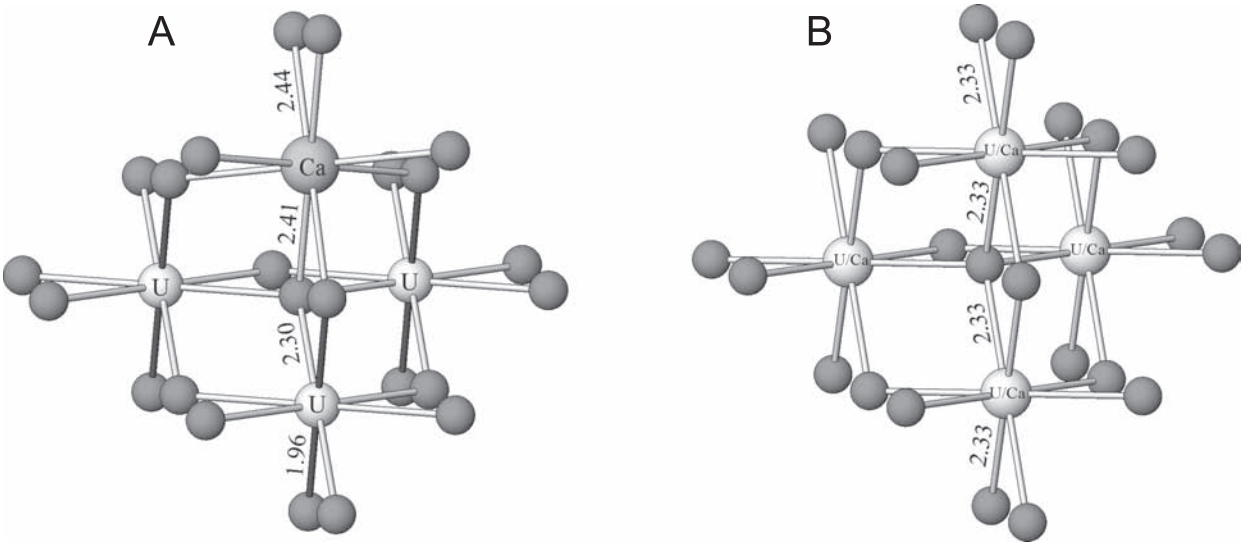

Figure 6. (**a**) Diagram illustrating distorted eightfold oxygen coordination of U^{6+}, characteristic of the uranyl group in synthetic rhombohedral $CaUO_4$ (Loopstra and Rietveld 1969). (**b**) Diagram illustrating cubic oxygen coordination of U^{6+} in vorlanite in averaged structure from the X-ray refinement.

× *U*) for rhombohedral $CaUO_4$ (Loopstra and Rietveld 1969). Given the evidence indicating the presence of the uranyl ion in the Raman spectra (Fig. 5), we suggest that there is also "uranyl disorder" in vorlanite, i.e., the short O-U-O body diagonal of 2 × 1.98 Å, characteristic of the uranyl group, is randomly aligned parallel to one of the four symmetry-equivalent body diagonals of the cube. The half unit-cell volume of vorlanite, 77.92 $Å^3$, exceeds the volume of a unit cell of rhombohedral $CaUO_4$, 76.26 $Å^3$ (Loopstra and Rietveld 1969), a relationship that is expected when comparing disordered and ordered structures. A consequence of the difference in cell volume is also the higher density (7.45 g/cm^3) of rhombohedral $CaUO_4$ (Loopstra and Rietveld 1969) compared to 7.29 g/cm^3 for vorlanite.

Burns et al. (1997) derived revised bond-valence parameters for U^{6+} that took into consideration the proper modeling of the uranyl group and was applicable to all coordination geometries of O. In rhombohedral $CaUO_4$ (Loopstra and Rietveld 1969) there are two symmetry independent O sites (O1 and O2, both four-coordinated). O1 is bonded 3 × to Ca (2.438 Å) and 1 × U (1.964 Å) yielding a bond valence sum of 2.01 v.u.; O2 is bonded 1 × to Ca (2.412 Å) and 3 × U (2.298 Å) yielding a bond valence sum of 2.19 v.u. If we use the Raman derived distance of 1.98 Å characteristic of the uranyl group in vorlanite, these two short U-O distances yield a contribution of 2.26 v.u. (1.13 v.u. each) leaving (6–2.26)/6 = 0.623 v.u. for each of the six long U-O bonds, which corresponds to 2.281 Å. With an approximate bond valence of 0.28 v.u. for a Ca-O bond in vorlanite (derived from rhombohedral $CaUO_4$) we may predict the local cation neighbors of fourfold coordinated O in vorlanite. Of course, the most balanced oxygen valence sums would be obtained for an ordered structure with O either coordinated to 3 × Ca and 1 × U (short U-O) or to 3 × U (long U-O) and 1 × Ca (like in rhombohedral $CaUO_4$) yielding an oxygen bond valence sum of 1.97 and 2.15 v.u., respectively. However, this Ca, U distribution pattern must rather be an exception because Ca, U order is not in agreement with the cubic structure of vorlanite. Any other combination of bonds to four-coordinate O yields strong deviation from the ideal oxygen bond valence sum of 2 v.u. Two examples: O bonded to 2 × U (long U-O) and 2 × Ca yields 1.81 v.u.; O bonded to 2 × U (long and short U-O) and 2 × Ca yields 2.31 v.u. In other words, U,Ca disorder leads to substantial bond valence strain in vorlanite.

Formation of vorlanite can be related to the progressive stage of skarn evolution, when rhombohedral ordered $CaUO_4$ formed first, which at higher temperature transformed to vorlanite. This transition is accompanied by a significant volume increase. The open question is: why did not vorlanite invert to rhombohedral $CaUO_4$ or what did stabilize the cation disordered structure of vorlanite?

Experimental data show that in the system CaO-UO_2 at temperatures higher than 1100 °C, even in presence of free oxygen, rhombohedral $CaUO_4$ becomes unstable due to the reduction of U^{6+} to U^{4+} and decomposes either to cubic $U_{1-\delta}Ca_\delta O_{2-\delta}$ or monoclinic perovskite $CaUO_3$ (Pialoux and Touzelin 1998). It is interesting that at a temperature higher than 1300–1400 °C CaU_2O_6, containing only U^{5+} with fluorite-type structure and cell dimention a = 5.37 Å, very close to the vorlanite cell dimension a = 5.38 Å, was synthesized (Herrero and Rijas 1988; Gómez-Rebollo et al. 1997).

Primary minerals in the skarn associated with vorlanite crystallized at high temperatures between 800–1000 °C and shallow depth (low pressure) (Gazeev et al. 2006; Galuskin et al. 2008). Rhombohedral $CaUO_4$, the vorlanite precursor, most likely crystallized later than primary larnite, rondorfite, and wadalite, and probably almost simultaneously with Ca-humites (Fig. 2b). Accessory zircon from the ignimbrites of the Upper Chegem volcanic structure is the most likely U source for $CaUO_4$.

Perhaps, a reason for the formation of vorlanite from rhombohedral $CaUO_4$ is the high radioactivity associated with the mechanical deformation of rhombohedral $CaUO_4$ crystals (Fig. 2). One may assume, that the Upper Chegem caldera with an age of ~2.8 Ma, estimated from the age of ignimbrites, formed during 50 000 years (Lipman et al. 1993; Gazis et al. 1995). Simultaneously, mechanical strain accumulated and radiation damage began to destabilize rhombohedral $CaUO_4$. The cumulative dose (α-decay events/mg) for vorlanite was calculated using following equation (Ewing et al. 2000): $D\alpha = 8N_1[\exp(\lambda_1 t) - 1] + 7N_2[\exp(\lambda_2 t) - 1] + 6N_3[\exp(\lambda_3 t) - 1]$, where N_1, N_2, N_3 are the actual values of ^{238}U, ^{235}U, and ^{232}Th, respectively in atoms/mg; λ_1, λ_2, and λ_3 are the decay constants for ^{238}U, ^{235}U, and ^{232}Th, respectively, in $years^{-1}$; and t is the estimated age (in years) of the ignimbrites [~2.8 Ma according to Lipman et al. (1993), Gazis et al. (1995)], coeval with vorlanite. The final dose expressed in displacement per atom (dpa) is calculated according to the equation: $\text{Dose (dpa)} = 9.40 \times 10^5 \times D\alpha \times M/(N_A \times 6)$, where M is the molar mass of the vorlanite and N_A is Avogadro's number. The cumulative dose of vorlanite = 6.30×10^{15} α-decay events/mg, which is equivalent of a dose of 0.56 dpa. Associated with vorlanite is the uranian garnet–elbrusite-(Zr) that, in contrast to vorlanite, completely lost the crystalline structure with a dose of ~0.25 dpa (Galuskina et al. 2010b).

Based on the foregoing interpretation, we suggest that radiation damage by α-decay events of U stressed the structure of rhombohedral CaUO4, resulting in atomic displacements that finally led to cation disorder and formation of the fluorite-type structure. Fluorite-type structures were also observed in complex oxides of pyrochlore-type ($A_2B_2O_7$) and muratoite ($A_6B_{12}C_4TX_{40-x}$) formed as a result of α-decay radiation damage (ion beam simulation) (Lian et al. 2005; Ewing 2005). The well-known radiation tolerance of fluorite-type structures (Sickafus et al. 2000) such as vorlanite helps explain why vorlanite persists as a crystalline compound, whereas rhombohedral $CaUO_4$ (apparently) does not.

Acknowledgments

The authors thank R. Finch for his careful review, which improved an early version of the manuscript. Special thanks are due to Ed Grew who handled the manuscript as Associate Editor. The work was partly supported by the Ministry of Science and Higher Education of Poland, grant no. N307 100238 and by the Russian Foundation of Basic Researches, Project 08-05-00181.

References cited

Allen, G.C. and Griffiths, A.J. (1979) Vibrational spectroscopy of alkaline-earth metal uranate compounds. Journal of the Chemical Society, Dalton Transactions, 315–319. DOI: 10.1039/DT9790000315

Allen, G.C., Griffiths, A.J., and Lee, B.J. (1978) X-ray photoelectron spectroscopy of alkaline earth metal uranate complexes. Transition Metal Chemistry, 3, 229–233.

Bartlett, J.R. and Cooney, R.P. (1989) On the determination of uranium-oxygen

bond lengths in dioxouranium (VI) compounds by Raman spectroscopy. Journal of Molecular Structure, 193, 295–300.
Belle, J. (1961) Uranium Dioxide: Properties and Nuclear Applications. U.S. Government Printing Office.
Bera, S., Sali, S.K., Sampath, S., Narasimhan, S.V., and Venugopa, V. (1998) Oxidation state of uranium: an XPS study of alkali and alkaline earth uranates. Journal of Nuclear Materials, 255, 26–33.
Burns, P.C. (1999) The crystal chemistry of uranium. In P.C. Burns and R. Finch, Eds., Uranium: Mineralogy, geochemistry and the environment, vol. 38, p. 23–90. Reviews in Mineralogy, Mineralogical Society of America, Chantilly, Virginia.
Burns, P.C. (2005) U^{6+} minerals and inorganic compounds: insights into an expanded structural hierarchy of crystal structures. Canadian Mineralogist, 43, 1839–1894.
Burns, P.C., Ewing, R.C., and Hawthorne, F.C. (1997) The crystal chemistry of hexavalent uranium: Polyhedron geometries, bond-valence parameters, and polymerization of polyhedra. Canadian Mineralogist, 35, 1551–1570.
Chadwick, D. (1973) Uranium 4f binding energies studied by X-ray photoelectron spectroscopy. Chemical Physics Letters, 21, 291–294.
Collela, M., Lumpkin, G.R., Zhang, Z., Buck, E.C., and Smith, K.L. (2005) Determination of uranium valence state in the brannerite structure using EELS, XPS, and EDX. Physics and Chemistry of Minerals, 32, 52–64.
Ewing, R.C. (2005) Plutonium and "minor" actinides: safe sequestration. Earth and Planetary Science Letters, 229, 165–181.
Ewing, R.C., Meldrum, A., Wang, L., and Wang, S. (2000) Radiation-induced amorphization. In S.A.T. Redfern and M.A. Carpenter, Eds., Transformation Process in Minerals, vol. 39, p. 319–361. Reviews in Mineralogy and Geochemistry, Mineralogical Society of America, Chantilly, Virginia.
Galuskin, E.V., Gazeev, V.M., Armbruster, T., Zadov, A.E., Galuskina, I.O., Pertsev, N.N., Dzierżanowski, P., Kadiyski, M., Gurbanov, A.G., Wrzalik, R., and Winiarski, A. (2008) Lakargiite $CaZrO_3$: A new mineral of the perovskite group from the North Caucasus, Kabardino-Balkaria, Russia. American Mineralogist, 93, 1903–1910.
Galuskin, E.V., Gazeev, V.M., Lazic, B., Armbruster, T., Galuskina, I.O., Zadov, A.E., Pertsev, N.N., Wrzalik, R., Dzierzanowski, P., Gurbanov, A.G., and Bzowska, G. (2009) Chegemite $Ca_7(SiO_4)_3(OH)_2$—A new humite-group calcium mineral from the Northern Caucasus, Kabardino-Balkaria, Russia. European Journal of Mineralogy, 21, 1045–1059.
Galuskina, I.O., Lazic, B., Armbruster, T., Galuskin, E.V., Gazeev, V.M., Zadov, A.E., Pertsev, N.N., Jeżak, E., Wrzalik, R., and Gurbanov, A.G. (2009) Kumtyubeite $Ca_5(SiO_4)_2F_2$—A new calcium mineral of the humite group from Northern Caucasus, Kabardino-Balkaria, Russia. American Mineralogist, 94, 1361–1370.
Galuskina, I.O., Galuskin, E.V., Armbruster, T., Lazic, B., Dzierżanowski, P., Gazeev, V.M., Prusik, K., Pertsev, N.N., Winiarski, A., Zadov, A.E., and others (2010a) Bitikleite-(SnAl) and bitikleite-(ZrFe)—New garnets from xenoliths of the Upper Chegem volcanic structure, Kabardino-Balkaria, Northern Caucasus, Russia. American Mineralogist, 95, 959–967.
Galuskina, I.O., Galuskin, E.V., Armbruster, T., Lazic, B., Kusz, J., Dzierżanowski, P., Gazeev, V.M., Pertsev, N.N., Prusik, K., Zadov, A.E., and others (2010b) Elbrusite-(Zr)—A new uranian garnet from the Upper Chegem caldera, Kabardino-Balkaria, Northern Caucasus, Russia. American Mineralogist, 95, 1172–1181.
Galuskina, I.O., Galuskin, E.V., Dzierżanowski, P., Gazeev, V.M., Prusik, K., Pertsev, N.N., Winiarski, A., Zadov, A.E., and Wrzalik, R. (2010c) Toturite $Ca_3Sn_2Fe_2SiO_{12}$—A new mineral species of the garnet group. American Mineralogist, 95, 1305–1311.
Gazeev, V.M., Zadov, A.E., Gurbanov, A.G., Pertsev, N.N., Mokhov, A.V., and Dokuchaev, A.Ya. (2006) Rare minerals of Verkhniy Chegem caldera (in skarned carbonates xenoliths in ignimbrites). Vestnik Vladikavkazskogo Nauchnogo Tsentra, 6, 18–27 (in Russian).
Gazis, C.A., Lanphere, M., and Taylor, H.P. (1995) $^{40}Ar/^{39}Ar$ and $^{18}O/^{16}O$ studies of the Chegem ash-flow caldera and the Eldjurta Granite: Cooling of two Pliocene igneous bodies in the Greater Caucasus Mountains, Russia. Earth and Planetary Science Letters, 134, 377–391.
Gómez-Rebollo, E., Herrero, P., and Rijas, R.M. (1997) Microstructural characterization of the stabilized fluorite phases formed in the $Ca_{1-y}La_yU_2O_{6+x}$ ($0 \le y \le 0.8$) system. Journal of Nuclear Materials, 245, 161–168.
Grenthe, I., Drożdżyński, J., Fujino, T., Buck, E.C., Albrecht-Schmitt, T.E., and Wolf, S.F. (2006) Uranium. In L.R. Morss, N.M. Edelstein, J. Fuger, and J.J. Katz, Eds., The Chemistry of the Actinide and Transactinide Elements, p. 253–298. Springer, The Netherlands.
Herrero, M.P. and Rijas, R.M. (1988) Substitution of Ca for La ions in the U-Ca mixed oxides: Effects on thermal stability of the fluorite phase. Journal of Solid State Chemistry, 73, 536–543.
Hoekstra, H.R. (1965) Infrared spectra of some alkali metal uranates. Journal of Inorganic and Nuclear Chemistry, 27, 801–808.
Janeczek, J. and Ewing, R.C. (1992) Structural formula of uraninite. Journal of Nuclear Materials, 190, 128–132.
Lian, J., Wang, L.M., Ewing, R.C., Yudintsev, S.V., and Stefanovsky, S.V. (2005) Thermally induced phase decomposition and nanocrystal formation in murataite ceramics. Journal of Materials Chemistry, 15, 709–714.
Liegeois-Duyckaerts, M. (1977) Infrared and Raman spectrum of $CaUO_4$: New data and interpretation. Spectrochimica Acta Part A: Molecular Spectroscopy, 6–7, 709–713.
Lipman, P.W., Bogatikov, O.A., Tsvetkov, A.A., Gazis, A.G., Gurbanov, A.G., Hon, K., Koronovsky, N.V., Kovalenko, V.I., and Marchev, P. (1993) 2.8 Ma ash-flow caldera at Chegem River in the northern Caucasus Moutains (Russia): Contemporaneous granites, and associated ore deposits. Journal of Volcanology and Geothermal Research, 57, 85–124.
Liu, J.-H., Van den Berghe, S., and Konstantinović, M.J. (2009) XPS spectra of the U^{5+} compounds KUO_3, $NaUO_3$ and $Ba_2U_2O_7$. Journal of Solid State Chemistry, 182, 1105–1108.
Loopstra, B.O. and Rietveld, H.M. (1969) The structure of some alkaline-earth metal uranates. Acta Crystallographica, B25, 787–791.
Matar, S.F. and Demazeau, G. (2009) Electronic band structure of $CaUO_4$ from first principle. Journal of Solid State Chemistry, 182, 2678–2684.
Ohwada, K. (1970) Uranium-oxygen lattic vibration of alkali monouranates. Spectrochimica Acta, 25A, 1723–1730.
Pialoux, A. and Touzelin, B. (1998) Étude du système U-Ca-O par diffractométrie de rayons X à haute temperature. Journal of Nuclear Materials, 255, 14–25.
Roof, I.P., Smith, M.D., and zur Loye H.-C. (2010) Crystal growth of K_2UO_4 and Na_4UO_5 using hydroxide fluxes. Journal of Crystal Growth, 312, 1240–1243.
Schindler, M., Hawthorne, F.C., Freund, M.S., and Burns, P.C. (2009) XPS spectra of uranyl minerals and synthetic uranyl compounds. I: The U 4f spectrum. Geochimica et Cosmochimica Acta, 73, 2471–2487.
Senanayake, S.D., Rousseau, R., Colegrave, D., and Idriss, H. (2005) The reaction of water on polycrystalline UO_2: Pathways to surface and bulk oxidation. Journal of Nuclear Materials, 342, 179–187.
Shannon, R.D. (1976) Revised effective ionic radii and systematic studies of interatomic distances in halides and chalcogenides. Acta Crystallographica, A32, 751–767.
Sickafus, K.E., Minervini, L., Grimes, R.W., Valdez, J.A., Ishimaru, M., Li, F., McClellan, K.J., and Hartmann, T. (2000) Radiation tolerance of complex oxides. Science, 289, 748–751.
Van den Berghe, S., Laval, J.-P., Gaudreau, B., Terryn, H., and Verwerft, M. (2000) XPS investigation on cesium uranates: Mixed valency behaviour of uranium. Journal of Nuclear Materials, 277, 28–36.
Volkovich, V.A., Griffiths, T.R., Fray, D.J., and Fields, M. (1998) Vibrational spectra of alkali metal (Li,Na and K) uranates and consequent assignment of uranate ion site symmetry. Vibrational Spectroscopy, 17, 83–91.
Volkovich, V.A., Griffiths, T.R., and Thied, R.C. (2001) Raman and infrared spectra of rubidium and caesium uranates (VI) and some problems assigning diuranate site symmetry. Vibrational Spectroscopy, 25, 223–230.
Zachariasen, W.H. (1948) Crystal Chemical Studies of the 5f-series of Elements. IV. The Crystal Structure of $Ca(UO_2)O_2$ and $Sr(UO_2)O_2$. Acta Crystallographica, 1, 281–285.
Zadov, A.E., Gazeev, V.M., Pertsev, N.N., Gurbanov, A.G., Yamnova, N.A., Gobechiya, E.R., and Chukanov, N.V. (2008) Discovery and investigation of a natural analog of calcio-olivine (γ-Ca_2SiO_4). Doklady Earth Sciences, 9, 1431–1434.

Manuscript received May 25, 2010
Manuscript accepted August 1, 2010
Manuscript handled by Edward Grew